SQUID TEM method for geothermal resource exploration: a case study in Southern Sumatra, Indonesia

Michael S. Zhdanov, Alexander Gribenko, and Leif Cox, Consortium for Electromagnetic Modeling and Inversion, University of Utah, and TechnoImaging, USA
Keiichi Tanabe, Tsunehiro Hato, and Akira Tsukamoto, SUSTEC, Japan

Summary

Geothermal energy has become an attractive renewable source of energy around the globe. Developing effective geophysical methods for geothermal exploration is vital for studying these resources. It is well known that electric conductivity is an important indicator of the location of geothermal sources. The objective of the paper is to demonstrate the effectiveness of the new geophysical method based on the SQUID measurements of the controlled source time domain electromagnetic (SQUID TEM) data for geothermal resource exploration. We have deployed highly-sensitive SQUID magnetic sensors to study the geothermal sources in the Geothermal Project Area in Southern Sumatra, Indonesia. We have also developed a large-scale 3D inversion method for interpreting the collected SQUID TEM data and reconstructing 3D distribution of the resistivity of the subsurface Field data inversion revealed several conductive anomalies, which may correspond to geothermal targets.

Introduction

Geothermal systems are usually associated with volcanically active geological provinces characterized by complex geology. Therefore, developing effective geophysical methods for accurately mapping the geothermal system and reservoir is vital for studying these resources. Electric conductivity is an important indicator of the location of geothermal sources. Until recently, the magnetotelluric survey was the preferable method for the geoelectrical exploration of geothermal systems. In this paper, we present an alternative approach based on the use of highly-sensitive SQUID magnetic sensors and an electric bipole transmitter. SQUID sensors make it possible to measure the magnetic field generated by a bipole source with high accuracy for a wide time interval (Motoori et al., 2018). In addition, the SQUID sensors measure all three components of the magnetic B field instead of its time derivative, dB/dt, measured by the conventional induction coils. This ensures recording at a later time, corresponding to a greater depth of investigation.

We conducted a SQUID TEM survey at a geothermal field in the Southern Sumatra region onshore Indonesia. The survey consisted of a long transmitting electric bipole and forty observation points. The collected data included amplitudes of the three components of the magnetic B-field at 40 locations, along with their standard deviations at 33 time gates ranging from 2e-05 to 1.39 seconds. Figure 1 presents a map showing the locations of the electric bipole transmitter and SQUID receivers.

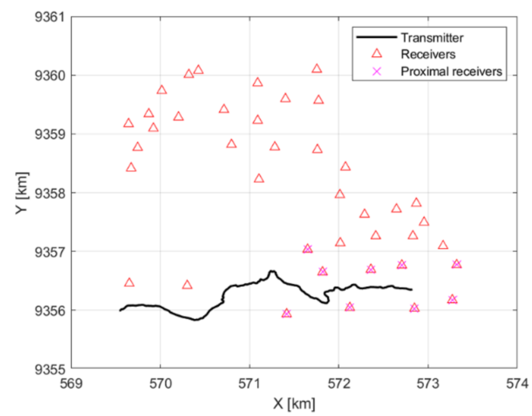

Figure 1: Map of the transmitter and receiver locations. Magenta crosses mark the receivers removed from the inversion.

We then applied 3D inversion to the observed SQUID TEM data, and the 3D model of the subsurface resistivity was generated, which corresponded well to the observed data.

3D inversion of SQUID TEM data

The goal of inversion is to recover the 3D resistivity distribution from the SQUID TEM data. However, SQUID TEM survey data are contaminated with noise, and the inverse model may change dramatically while keeping the predicted data within the noise level. This means that SQUID TEM inversion is ill-posed; i.e., solutions are nonunique and unstable (Zhdanov, 2002, 2015, 2018). One must use regularization to obtain a unique and stable solution. This can be achieved by minimization of the Tikhonov parametric functional, $P^{\alpha}(\boldsymbol{\sigma})$:

$$P^{\alpha}(\boldsymbol{\sigma}) = \|\boldsymbol{W}_d(\boldsymbol{A}(\boldsymbol{\sigma}) - \boldsymbol{d}_{obs}\|^2 + \alpha\left\|\boldsymbol{W}_{\boldsymbol{m}}(\boldsymbol{\sigma} - \boldsymbol{\sigma}_{apr})\right\|^2 \rightarrow min, \tag{1}$$

where $\boldsymbol{A}$ is the nonlinear forward modeling operator, $\boldsymbol{\sigma}$ is the vector of conductivities, $\boldsymbol{d_{obs}}$ is the vector of observed data, $\boldsymbol{\sigma_{apr}}$ is the of the a priori conductivities, and $\|\ldots\|$denotes the respective least-square norm. The minimization problem formulated by (1) was solved via re-weighted regularized conjugate gradient (RRCG) method (Zhdanov, 2002)

The 3D numerical forward modeling for this project was based on the integral equation method. This method has been covered extensively in the literature (e.g., Zhdanov 2002, 2009, 2018). The main advantage of this method is that only the area of interest needs to be discretized, not the entire domain. The conductivity is represented as a superposition of the background horizontally layered model and anomalous conductivity. The observed EM field is divided into a scattering or anomalous component and a background component. The background fields from the background conductivity are computed by the semi-analytical method. The anomalous fields are included separately, which increases the method's accuracy and decreases computation time.

Data and model weights are introduced to equation (1) through weighting matrices $\boldsymbol{W}_d$ and $\boldsymbol{W}_{\boldsymbol{m}}$ respectively. We used data weights as the inverse of the standard deviations to reduce the input of the noisy data into the inversion result. Model weighting matrices are selected based on their integrated sensitivity (Zhdanov, 2002). As a result, they provide equal sensitivity of the observed data to cells located at different depths and at different horizontal positions.

To reduce the dynamic range of the model parameters, we reformulate the inverse problem in logarithmic space. The geological constraints manifest themselves as regularization that can be quantified through a choice of data weights, model upper and lower bounds, model weights, an a priori model, and the type of stabilizing functional. The latter incorporates information about the class of models used in the inversion. The choice of stabilizing functional is based on the user's geological knowledge and prejudice. In this inversion, we used the first derivative stabilizer with adaptive regularization (Zhdanov, 2002).

All inversions were carried out using the developed EMVision® software package. The software uses a robust and stable method to solve for the 3D physical parameter distribution in the earth. Fast and accurate algorithms based on the integral equation method are used to model the physics, and flexibility in the software allows a wide selection of stabilizers, a priori models, and cooperative inversion techniques (Zhdanov, 2015). The inversion method uses data weights to ensure the fitting of the data to the appropriate noise level and model weights to normalize sensitivities of the data for increased depth resolution and stability.

SQUID TEM inversion results

The developed method of 3D inversion was applied to the SQUID TEM data collected over the AOI shown in Figure 1. The dimensions of the inversion domain were 7,000 by 8,000 by 3,500 m in X (Easting), Y (Northing), and Z (Elevation) directions. The domain extended from 567 km to 576 km UTM Easting (X), 9,353 km to 9,361 km UTM Northing (Y), and from 0 to approximately 3.5 km depth from the surface in the vertical direction. A uniform grid of 25 by 25 by 25 m cells was used in the modeling and inversion.

We used the best-fitting 25 Ohm-m half-space homogeneous model as a starting model for the 3D inversion. The regularized inversion required about one hundred iterations of the Regularized Re-weighted Conjugate Gradient (RRCG) minimization to find a solution. The inversion was terminated once the change of the misfit functional decreased to less than 0.1 % from one iteration to another. The inversion converged to a global RMS misfit χ^2 of 3.61, which is a very statistically reasonable value indicating a relatively low misfit level between the observed and predicted data. Figure 2 presents the distribution of the local RMS misfit for different stations.

Figure 4 shows an example of the vertical cross section of the 3D resistivity distribution recovered from unconstrained inversion of HeliTEM data along a profile. Figure 3 shows decay curves of the observed and predicted data to illustrate the SQUID TEM data fit.

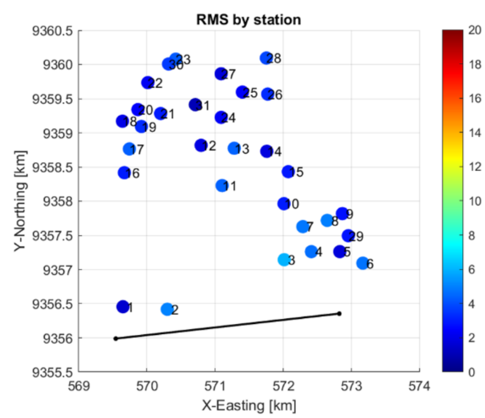

Figure 2: Station-by-station distribution of the local RMS misfit.

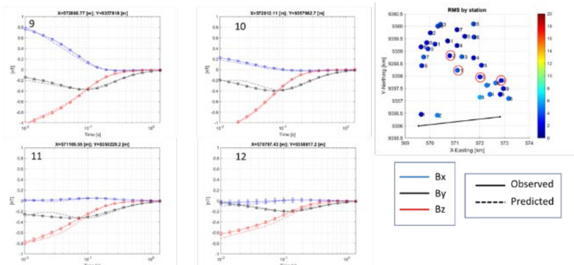

Figure 3: Observed (solid) and predicted (dashed) decay curves for the receivers 9 - 12.

Figure 4 represents a 3D view of the inversion result using isosurfaces at several resistivity values, 1, 10, and 100 Ohm-m. One can identify several near-surface conductive anomalies in the Northern region of the survey area. Two strong conductive structures are discovered in the South-Central area of the survey at depths between 500 and 1,000 m, approximately. Figure 5 shows a horizontal section at 700 m depth from the surface, which outlines the horizontal extent of the conductors. Figure 6 combines several vertical sections to provide a perspective view of the anomalies' extent in vertical and horizontal directions. Figure 7 shows the vertical section of the 3D resistivity model produced by the inversion of the SQUID TEM data.

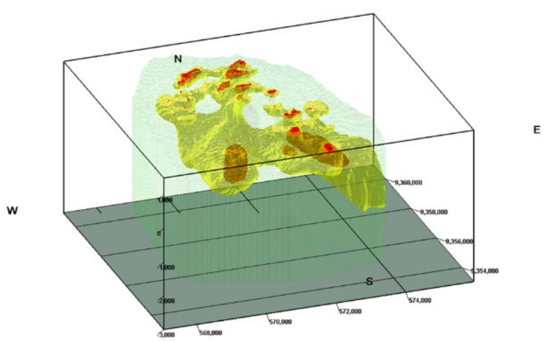

Figure 4: 3D view looking North-East of the inverse model represented by isosurfaces at 1, 10, and 100 Ohm-m shown by red, yellow, and green color, respectively.

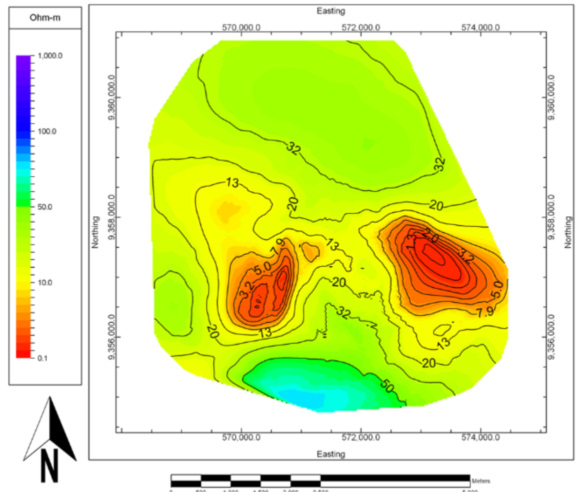

Figure 5: Horizontal section of the recovered resistivity model at 700 m depth.

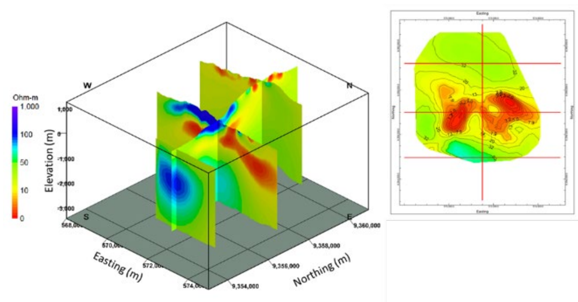

Figure 6: Combined vertical sections through the recovered resistivity distribution. Locations of the sections are shown on the map to the right.

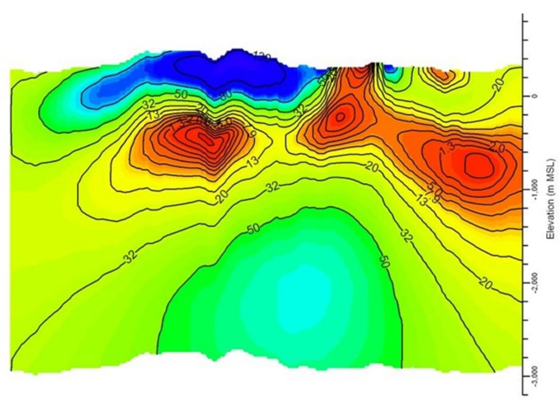

Figure 7: The vertical section of the 3D resistivity model produced by the inversion of the SQUID TEM data..

Inversion study of SQUID TEM survey in Raja Basa Geothermal Project Area

The 3D inverse resistivity model revealed several near-surface conductive anomalies in the Northern region of the survey area. The strong conductive structure was discovered in the South-Central area of the survey at depths between 500 and 1,000 m (Figure 7). This conductive zone indicates the geothermal source location. It has a resistivity of a few ohm-m, which is indicative of the high enthalpy reservoirs (T>~215°C) possibly formed by a clay cap that holds the hot fluid and keeps it from escaping to the surface. Beneath this highly conductive zone, at a depth of about 1 km, we observe a zone with resistivity values in the low double digits, representing the main geothermal reservoir possibly formed by the saline aquifer and host rocks rich in silica and epidote. This geoelectrical section represents a pattern typical for a high-temperature geothermal reservoir.

Conclusions

This paper presents new method of geothermal exploration based on SQUID magnetic receivers and controlled source transmitters. This method has significant advantages over the traditional magnetotelluric method by providing better resolution of geoelectrical structures due to the SQUID receivers' high sensitivity. By using the controlled source, we avoid the limitations of the MT method related to the plane-wave structure of the primary field. The developed 3D inversion method generates detailed 3D geoelectrical images of the subsurface from the SQUID data. These advances provide practicing geoscientists with new geophysical tool for exploring not only geothermal but mineral, oil, and gas deposits.

The two distinct deep conductors, possibly interconnected, were identified at depths between 500 and 1,000 m below the surface. The eastern conductor appears to have a surface expression roughly in the center of the inversion domain horizontally. These conductive zones may be considered indicators of the geothermal source locations. Thus, the SQUID TEM survey helped identify the deep conductive anomalies representing geothermal targets in the survey area.

Acknowledgments

The authors acknowledge SUSTEC, TechnoImaging, and the Consortium for Electromagnetic Modeling and Inversion (CEMI) of The University of Utah for the support of this project and permission to publish.

References

Motoori, S. Ueda, K. Masuda, E. Arai1, T. Hato, A. Tsukamoto, H. Watanab, H. Ishikawa, C. Okada, and T. Yamazak, 2018, A newly developed 3ch system of SQUITEM III and the result of its field test: Near Surface Geoscience, Conference and Exhibition of European Association of Geoscientists & Engineers (EAGE), Porto, Portugal.

Zhdanov, M. S., 2002, Geophysical inverse theory and regularization problems: Elsevier.

Zhdanov, M. S., 2009, Geophysical electromagnetic theory and methods: Elsevier.

Zhdanov, M. S., 2015, Inverse theory and applications in geophysics: Elsevier

Zhdanov, M. S., 2018, Foundations of geophysical electromagnetic theory and methods: Elsevier.